Adv. Theor. Appl. Mech., Vol. 3, 2010, no. 5, 233 - 252

Scaling Exponents of Structure Functions in an Eccentrically Rotating Flask

Vikram J. Kaku

Department of Mechanical Engineering
Temple University, Philadelphia, PA, USA
vkaku@temple.edu

Michel C. Boufadel

Department of Civil & Environmental Engineering
Temple University, 1947 N. 12th Street, Philadelphia, PA 19122, USA
boufadel@temple.edu

James W. Weaver

National Exposure Research Laboratory,
U.S. Environmental Protection Agency, Athens, GA, USA

Abstract

Velocity time series measurements were obtained using a hot-wire anemometer (HWA) in a Swirling flask eccentrically rotated by an orbital shaker. Two rotation speeds Ω were considered: 18.32 and 20.94 rad/s. Average azimuthal velocity distribution showed that the flow in the flask was quasi-two-dimensional at the large scale. Structure functions were obtained from the probability distribution functions (PDF) of the velocity differences in the spatial domain, viz. $S_p = \left\langle |\delta u|^p \right\rangle$. The scaling exponents ζ_p of these structure functions were obtained by using the Extended Self-Similarity (ESS) method. For high local Rossby numbers (i.e., as the flow becomes more three-dimensional), these exponents departed from the $p/3$ at high values of p and followed closely with the She-Leveque model of turbulence. The β-test of the

Hierarchical Structure (She-Leveque) model applied on our experimental data showed that values of β decreased with increase in rotation speeds and elevations; high β values correspond to highly intermittent flow. The γ-test of the Hierarchical Structure model confirmed the observations from the β-test. We conclude that the flow in the SF is three dimensional at the local scale while being quasi-two-dimensional at the large scale.

Keywords: Dispersants, Extended Self-Similarity, Hierarchical Structure model, Oil Spill, Structure Functions, Turbulence

1 Introduction

Dispersants are used to mitigate the spreading of oil spill to the shoreline, where the adverse effects of spill are more severe. These chemicals break the oil slick into droplets that penetrate deep in the sea due to the action of waves. This process is termed "dispersion" in the oil literature (to be distinguished from the spreading of chemicals due to the spatial variation of velocity such as presented by Taylor [34, 35], Fischer et al [15]). Dispersion of oil is a chemico-physical process that depends on both the type of dispersant/oil pair and the sea state. Small scale laboratory experiments are commonly used to test the effectiveness of dispersants due to ease in repeating such experiments and their relatively low cost. The Swirling flask (SF) test method [13 – 14] is a widely used small scale dispersant effectiveness test method. The test consists of placing a mixture of oil, seawater, and a dispersant in the SF positioned on an orbital (circular motion) shaker [10], then mixing the contents for a specified amount of time, allowing a short settling time, and then extracting the contents from the SF and measuring the concentration of oil dispersed in the water.

The goal of this study is to determine the statistical properties of turbulence in the SF. The measurement of these statistical properties will provide an insight into the relationship between intermittent structures in the flow and the scale dependence of the statistics.

In three-dimensional (3D) turbulence, vortices stretch and fold repeatedly until they collapse to intense filaments [16]. These filaments affect the transfer in the energy cascade, creating a rate of strong scale-dependence [16]. In addition, if one imagines the hot wire probe in the flow, vortex filaments while sweeping past the probe will yield intermittent bursts in the velocity measurements. This intermittency is an important characteristic property of 3D turbulence. To characterize the properties of fully developed turbulence, the structure functions $S_p(l)$ (viz. moments of the

velocity differences) on the spatial scale l are of special interest [11]. The pth-order structure function is defined as:

$$S_p(l) = \left\langle \left| \delta u_l \right|^p \right\rangle = \left\langle \left| u(x+l) - u(x) \right|^p \right\rangle \quad (1)$$

where l is the separation distance between two points and u is the velocity component in the azimuthal direction. Kolmogorov's 1941 theory (K41) [23] assumes self-similar statistics meaning that the rate of energy transfer is constant for all length scales, and that one cannot distinguish the dynamics at a selected length in the inertial sub-range from other lengths. Self similarity results in:

$$S_p(l) \sim l^{\zeta_p} \quad (2)$$

where $\zeta_p = p/3$. However, extensive experimental and numerical investigations have highlighted nonlinear dependence on p [1, 37], which is to due intermittency [28]. It is also a sign of scale-dependent flow statistics. This departure from K41 has been represented by a variety of conceptual models of turbulence [2, 7, 17, 21, 24, 27, 30]. Of interest in this work is the model of She-Leveque or Hierarchical Structure Model [31]. The HSM model predicts that the rate of energy transfer as a function of scale has a hierarchical symmetry, whereby intense "more intermittent" structures are related to weaker "less intermittent" structures. The details of this model are discussed in Section 5. The scaling exponent of the structure function derived by HSM model is [31]:

$$\zeta_p = \frac{p}{9} + 2\left[1 - (2/3)^{p/3}\right] \quad (3)$$

Eq. 3 shows that the scaling exponent is a nonlinear function of the moment's order p.

The layout of this paper is as follows: Section 2 covers the experimental set-up and details of the data collection. Section 3 describes the macro-scale flow characteristics in the SF. Section 4 gives results of the structure function exponents; Section 5 gives description of hierarchical structure model and results of its comparison with experimental data. Section 6 has the discussion of our results.

2 Experimental Set-up

The experimental setup (Fig. 1) consisted of 150-mL Swirling flask, SF, and an orbital shaker (3518, Lab-Line Instruments Inc.). This flask contained 120mL of tap water as the working fluid. The flask was held in place on the orbital shaker using flask holder. The diameter of the circle traced by the shaker was 1.9 cm. During rotation, the location of the flask was measured using a Position Transducer (PN150-0121, SpaceAge Control Inc.). The velocity time series was obtained using constant-temperature hot-wire anemometer, HWA (TSI model 1750) with the corresponding

probe (TSI model 1210-20W, single cylindrical sensor). The probe was mounted on the orbital shaker such that it rotated with the flask to measure flask water velocity in the azimuthal direction of the flow. Location and speed measurements were interfaced to a computer using a data-acquisition board, DAS 1401, by Keithley Instruments, Inc., (Cleveland, Ohio) with a built-in analog-to-digital circuit. The data logging software LABTECH Notebook Pro (Laboratory Technologies, Inc.) was used. The HWA is essentially an electric resistor that cools upon passage of water flow. The change in temperature alters the voltage that passes through the resistor. Hence, voltage reading across the HWA provides a surrogate measure of the water velocity. The HWA was calibrated in the velocity range [0-50 cm/s] using recirculating type water channel. Several factors influence the accuracy of the hot wire data: contaminants in the water, bubbles forming on the probes, and temperature drifts. These effects were reduced by refilling water in the flask everyday and replacing probes to control aging. The water was allowed to de-gas overnight to minimize the effects of bubble formation. Ambient temperatures were measured during the experiments and were verified to be within ±1°C. Furthermore, care was taken in aligning the probe when they were inserted in the flask; they were oriented radially so that they would measure azimuthal component of the flow. The output voltage from HWA at zero velocities varied from 2.8 to 2.89 volts throughout the duration of the experiments, which is less than 4%. Hence zero-drift was not a major problem.

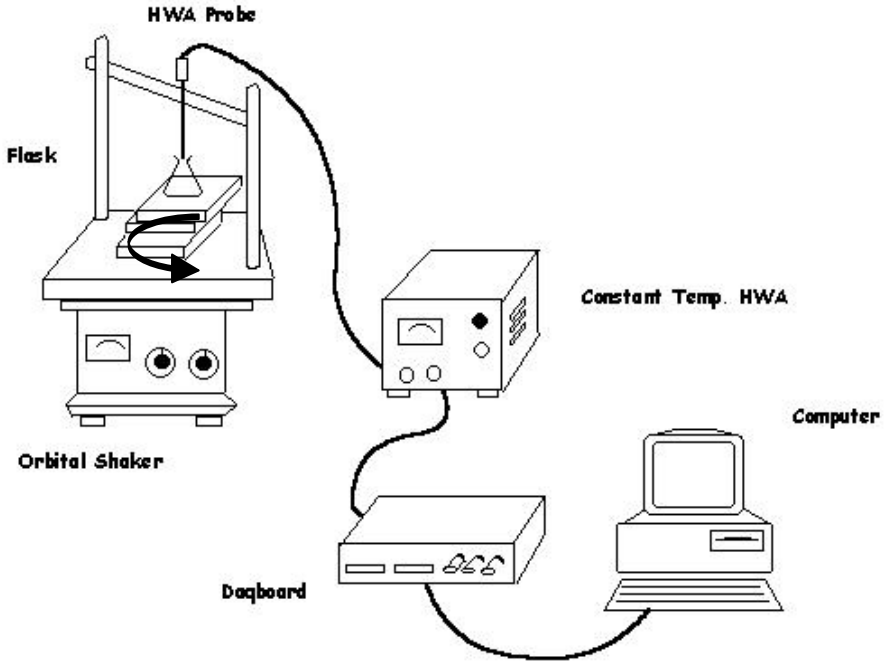

FIG. 1. Experimental Set-up

The velocities were measured in the center vertical plane of the SF (Fig. 2) at a spatial interval of 2mm in the horizontal (i.e. radial) direction and 5mm in the vertical direction. This totaled in 70 locations in the SF. The data collection frequency was 1,000 Hz. The sampling duration was 10 seconds for each location. This resulted in a time series of 10^4 data points for each location in the flask. Although one flask rotation took about 0.34 second at Ω=18.32 rad/s and 0.3 second at Ω=20.94 rad/s, the long measurement duration (10 seconds) was intended to increase the reliability of the experiments by having enough replicates: 29 replicates at 18.32 rad/s and 33 replicates at 20.94 rad/s. The increase of the number of replicates with the rotation speed is a welcome outcome, as the flow becomes more random with an increase in Ω, and a large number of replicates would minimize sampling errors.

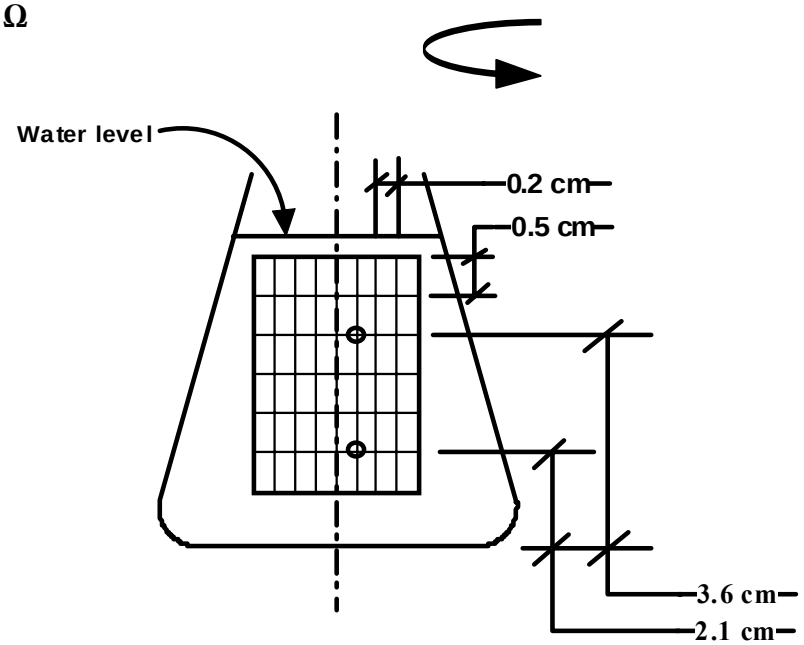

FIG. 2. Schematic of the Swirling Flask with the grid showing locations where azimuthal velocity was measured. The locations analyzed are marked O.

3 Flow Description

The azimuthal velocity measured in the SF at 70 locations was used to describe the large- scale flow pattern. The statistical properties of turbulence in the SF were evaluated at two locations at the same radial coordinates and separated by the vertical distance of 1.5cm (shown by circles in Fig. 2). These locations are close to the center of the flask to reduce boundary effects. The coordinates of these locations are X =

0.2cm, Z = 3.6cm, and X = 0.2cm, Z = 2.1cm; where X is the distance from the center of the flask, and Z is the elevation from the bottom of the flask. As the position of the orbital shaker corresponding to each velocity in the data series is known (from the position sensor), we report in Fig. 3 time series that start with the same location of the orbital shaker. Fig. 3 shows that the velocity peaks at the bottom are smaller than at the top and that they are lagging them. This decrease in magnitude is expected for free surface flows (e.g., waves that are generated by wind in the ocean) where maximum velocities occur near the surface.

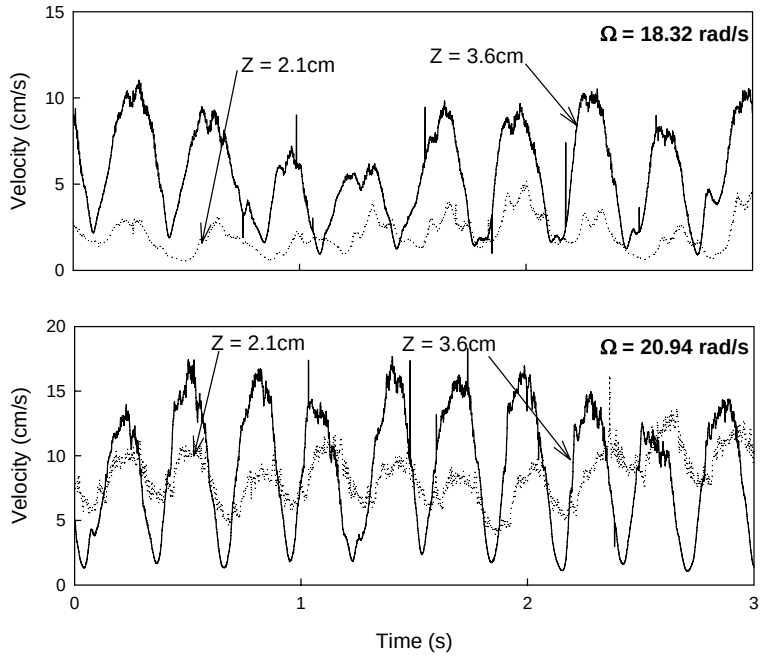

FIG. 3. Azimuthal velocity at the top and bottom locations of the SF at Ω = 18.32 and 20.94 rad/s.

3.1 Reynolds and Rossby numbers

The rotating flow can be described by two dimensionless numbers, the Reynolds number ($\mathrm{Re}=\frac{U L}{\nu}$), and the Rossby number ($Ro=\frac{U}{2\Omega L}$). These numbers were evaluated in the SF as reported in Table 1. Values of the Reynolds and Rossby numbers for the hot wire data corresponding to different locations and orbital shaker speeds are given in Table 1. A decrease in the Rossby number indicates that the flow is becoming more two-dimensional (in the horizontal). The increase of Ro with Ω observed in some cases in this work might be surprising, because one intuitively expects the flow to become more two-dimensional as Ω increases. However, the

flask walls are not vertical (Figure 2) and a free surface is present. Also we noted that as Ω increased, the height of the rotating gravity wave increased (which is to be expected). If one treats this wave based on the linear theory as an approximation then one notes that the vertical accelerations and forces are proportional to wave height [12].

Given that the Reynolds number is large, a decrease in Ro indicates also that turbulence is becoming more two-dimensional turbulence. This has important implications when interpreting the scaling of the structure functions below.

TABLE 1: Values of Parameter and Dimensionless Numbers Based on HWA Data.

No.	Rotation Ω, rad/s	Elevation Z, cm	Integral length scale L, cm	Average Velocity U, cm/s	Reynolds no.Re	Rossby no. Ro
1	18.32	3.6	4.2	7.15	3006	0.046
2	18.32	2.1	5	2.48	1240	0.013
3	20.94	3.6	4.2	11.26	4731	0.064
4	20.94	2.1	5	8.58	4290	0.040

3.2 Average Azimuthal Velocity Distribution

The average azimuthal velocity distribution for both rotations, Ω = 18.32, and 20.94 rad/s, was obtained by taking the average over 10 seconds of the time series at each measurement location. The contours of these average velocities are shown in Fig. 4. The sense of the azimuthal velocity is in the direction of rotation of the orbital shaker. The contours in the SF appear to be symmetric (within experimental errors) with respect to the center axis with relatively low velocities occupying the central portion of the flask. At the large scale, it can be the loosely said that the flow in the SF has a "stagnant core" due to solid body rotation and appears to be quasi-two-dimensional along its axis of symmetry.

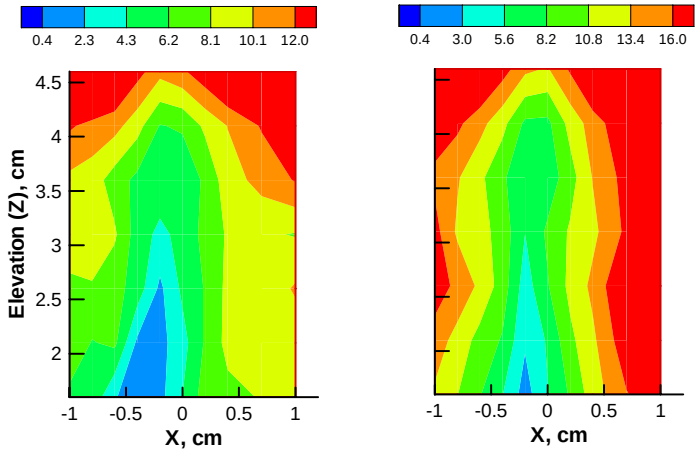

FIG. 4. Contours of average azimuthal velocities in the SF at orbital shaker speeds, Ω = 18.32 (left) and 20.94 rad/s (right).

3.3 Energy Spectra

To calculate energy spectra, velocity time series data were converted to spatial record assuming Taylor's frozen turbulence hypothesis as conducted by [29]. This was done by cumulatively summing over the velocities, then finding the corresponding spatial position for each time step, and finally interpolating onto an equally spaced data series. This was applicable because turbulent intensity $Tu = \sqrt{\langle u^2 \rangle}/U \leq 10\%$ (in our experiments, Tu = 4- 6%) [26]. The spectra obtained from these velocity space series are shown in Fig. 5. Also, the average spectra were computed by averaging the spectral amplitudes at all locations corresponding to the same frequencies. The individual spectra shown in Fig. 5 were similar to average spectra and hence representative of the complete flask at corresponding orbital shaker speeds. The spectra of turbulent flows have inertial sub-range which scales according to Kolmogorov's prediction of $E(k) \sim k^{-5/3}$ [22]. The spectra shown in Fig. 5 have a linear region whose slope is steeper than -5/3, which is due to the rotational motion of the flow, as observed in prior studies [5, 9, 18, 33, 38].

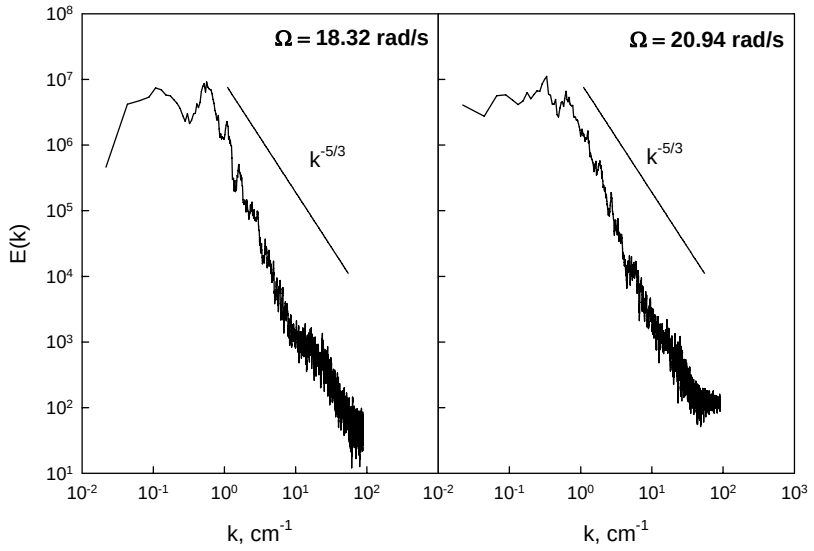

FIG. 5. Energy spectra in the SF for rotation speeds of Ω = 18.32, 20.94 rad/s

4 Structure Functions

4.1 Kolmogorov scale

The Kolmogorov scale, η, provides an estimate of the smallest eddy that can exist prior to the dissipation by (molecular) viscous friction. It is given by the fluid viscosity and the energy dissipation rate ε [36, Chapter 3]:

$$\eta = \left(\frac{\nu^3}{\varepsilon} \right)^{1/4} \tag{4}$$

The evaluation of ε in this study is done by using autocorrelation approach. The details of this method are covered by [19, 20]. The estimated values of η were 0.032cm and 0.024cm for Ω = 18.32, and 20.94 rad/s, respectively. The digital sampling rate of the hot wire probe, $f = 10^3$ Hz, corresponds to the spatial scale of $U / f \approx 0.011$ cm, which is smaller than η values. Hence, the measurements of the hot wire allowed proper evaluation of η.

4.2 Scaling exponents of structure functions

The azimuthal velocity data series on the length scale (obtained in Section 3.3) was used to obtain structure functions. The following method was used to compute the structure functions [32]: First a histogram of the velocity increments δu_l was constructed. It was then normalized to make it a probability distribution function

(PDF), $P(\delta u_l)$. The structure functions were then evaluated by direct integration of the PDF's using the following equation:

$$S_p(l) = \int_{-\infty}^{\infty} |\delta u_l|^p P(\delta u_l) d(\delta u_l) \tag{5}$$

The Simpson's rule [25] was used to numerically integrate the PDF's. This method of obtaining $S_p(l)$ is fast to implement, and is less sensitive to erroneous measurements than using the raw data for velocity differences [32]. The structure function exponents ζ_p were obtained by the method of Extended Self Similarity (ESS). This technique, introduced by Benzi et al. [6], has become the standard way to extract scaling exponents from flows where the scaling range is limited. It works by plotting S_p vs. S_3 on a log-log plot and fitting a straight line through them. The underlying idea is that the slope of log S_p vs. log S_3 yields ζ_p / ζ_3 and as $\zeta_3 = 1$, the slope gives ζ_p [23]. The technique minimizes systematic errors (or trends) that could be present in S_p, because the same trend would be present in S_3. A representative plots of $\log S_p$ vs. $\log S_3$ for the flow in the SF for Ω = 18.32, and 20.94 rad/s are shown in Fig. 6. The fits were good for both Ω conditions for length scales of $0.08 < l < 0.9$cm in the case of Ω = 18.32 rad/s, and $0.05 < l < 0.9$cm in the case of Ω = 20.94 rad/s. The scaling region was bounded by the Kolmogorov scale η at the lower end and by the integral length scale L at the higher end, but never quite reached those scales.

The structure function exponents ζ_p are shown in Fig. 7 for $p \leq 10$. The straight dashed line has the slope of 1/3 representing the K41 prediction. The curved continuous line corresponds to the She-Leveque model of intermittency given by Eq. (3) and will be discussed in Section 5. The theoretical values of ζ_p agree quite well with the experimental values up to $p = 7$. Some of the discrepancy above $p = 7$ may be attributed to less reliable statistics because as the values of p increases, large values of $|\delta u_l|^p$ which are expectedly scarce (the notion of an outlier could be recalled here) dominate the remaining values.

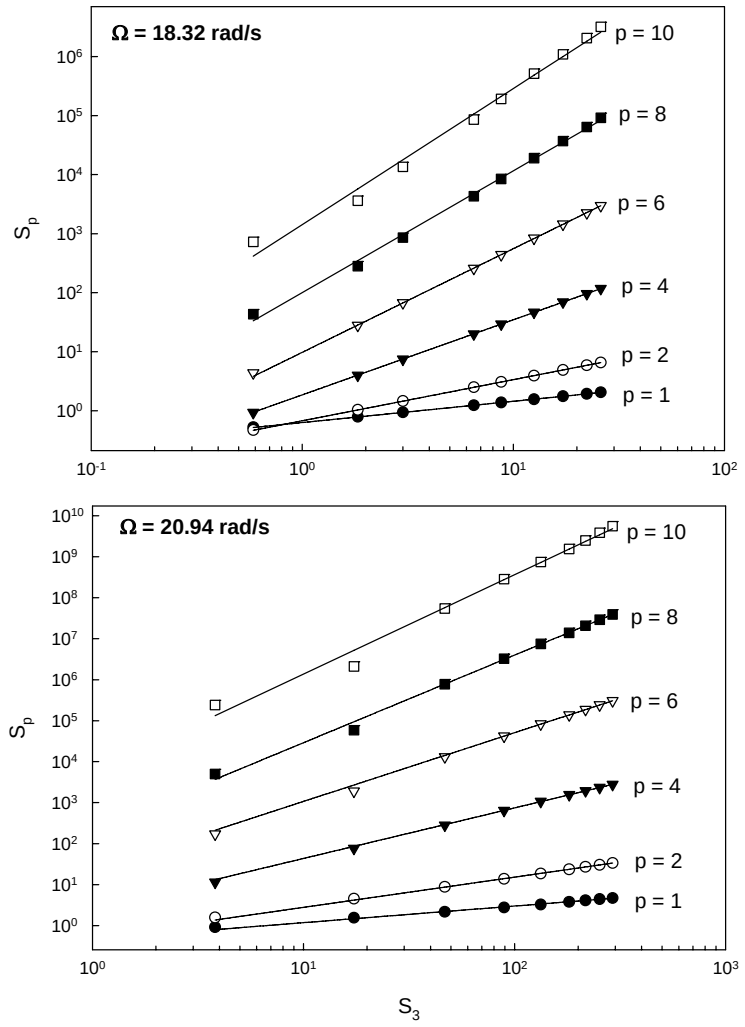

FIG. 6. Extended Self Similarity (ESS) plots for the flow in the SF for rotation speeds of Ω = 18.32, 20.94 rad/s

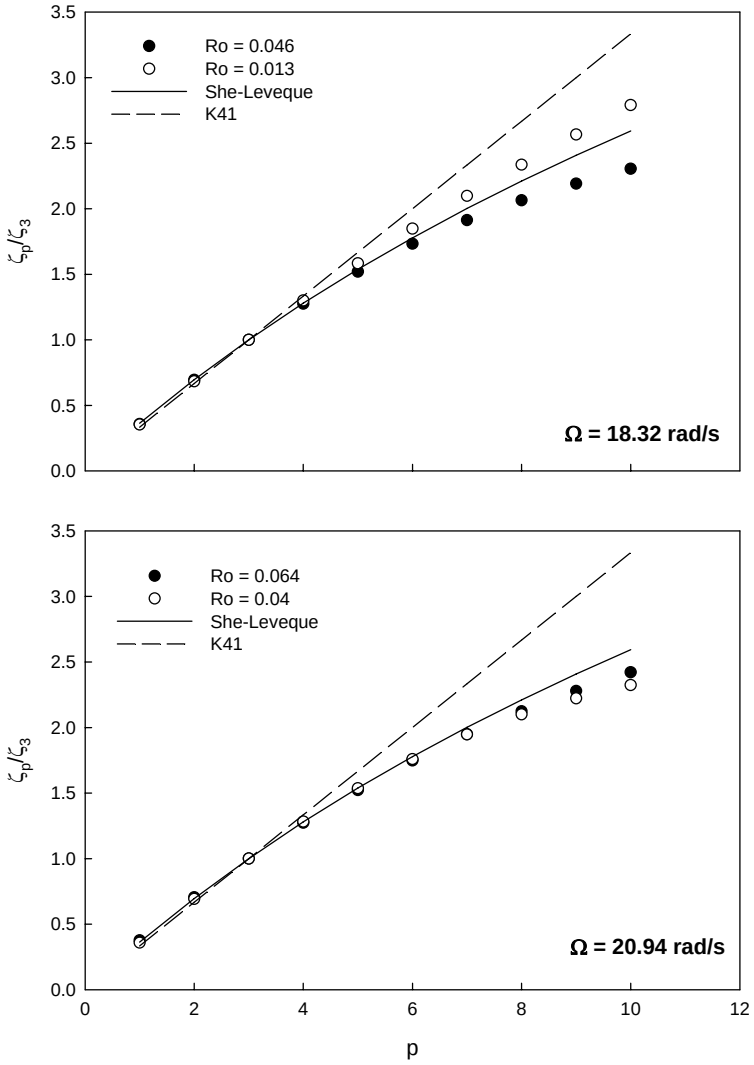

FIG. 7. Structure function exponent ratio as a function of order *p* for flows in Table 1.

The scaling for low Rossby number (i.e, high rotation), Ro = 0.013, followed much closer to the *p/3* line than that for high Rossby number. This is understandable because as the Rossby number decreases the flow approaches two-dimensional turbulence, whose theoretical scaling is *p/3*. The She-Leveque curve represents three-dimensional turbulence, as confirmed by direct numerical solutions (DNS) of the Navier-Stokes equations and experimental data [3, 8].

5 Hierarchical Structure Model

To further understand the internal structure of the flow (e.g., intermittency), we compared our experimental results with the She-Leveque or Hierarchical structure model of turbulence [31]. This model proposes two tests (the β-test and the γ-test) of the internal organization of flow structures, which resulted in better understanding of relationship between structures which are highly intermittent and the ones which are weaker. The test characterizes velocity increments δu_l by a hierarchy of fluctuation structures: $F_p(l)$ (p = 0, 1, 2 …) defined by the ratio of the successive structure functions $S_{p+1}(l)/S_p(l)$. The intensity of the pth order velocity increment structures $F_p(l)$ is given by:

$$F_p(l)=\frac{S_{p+1}(l)}{S_p(l)}=\frac{\int|\delta u_l|^{p+1}P(\delta u_l)\,d\delta u_l}{\int|\delta u_l|^{p}P(\delta u_l)\,d\delta u_l}=\int \delta u_l\,Q_p(\delta u_l)\,d\delta u_l \tag{6}$$

where $Q_p(\delta u_l)$ is the weighted PDF for which the function $F_p(l)$ is the mathematical expectation given by:

$$Q_p(\delta u_l)=|\delta u_l|^{p}P(\delta u_l)/\int|\delta u_l|^{p}P(\delta u_l)\,d\delta u_l \tag{7}$$

For higher p, $Q_p(\delta u_l)$ peaks at high intensity of fluctuations of δu_l and hence functions $F_p(l)$ describe the intensity of fluctuations in the flow [4]. This model postulates the scaling behavior as follows:

$$F_{p+1}(l)=A_pF_p(l)^{\beta}F_{\infty}(l)^{1-\beta} \tag{8}$$

where A_p are constants which are independent of l, the exponent β ($0 \le \beta \le 1$) is a constant, and the function F_∞ describes the most intermittent, highest intensity fluctuations.

5.1 The β-test

The difficulty of waiting infinite time to measure F_∞ is avoided by considering the ratio [4]:

$$\frac{F_{p+1}(l)}{F_p(l)}=\frac{A_p}{A_1}\left(\frac{F_p(l)}{F_1(l)}\right)^{\beta} \tag{9}$$

The β-test consists of checking for this power law scaling. If it exists, then the hierarchical symmetry is verified, and the value of the slope β in log-log space describes the amount of intermittency in the flow (β = 1 corresponds to non-intermittent flow and β = 0 is the highly intermittent flow). The plots of the β-test applied for the conditions in Table 1 are shown in Fig. 8. The value of β were smaller at the location Z = 3.1cm, which indicates that the flow was more intermittent at the

surface than that at the bottom of the flask. The values of β at Ω = 20.94 rad/s were smaller than that at Ω = 18.32 rad/s for corresponding locations, which indicate that the intermittency increased with the rotation speed of the orbital shaker. The points in Fig. 8 for *Ro*=0.013 fall in compact groups for each *p*, as expected for a self-similar flow; if the flow were perfectly self-similar, these compact groups would each collapse to a point since there is no dependence on *l*.

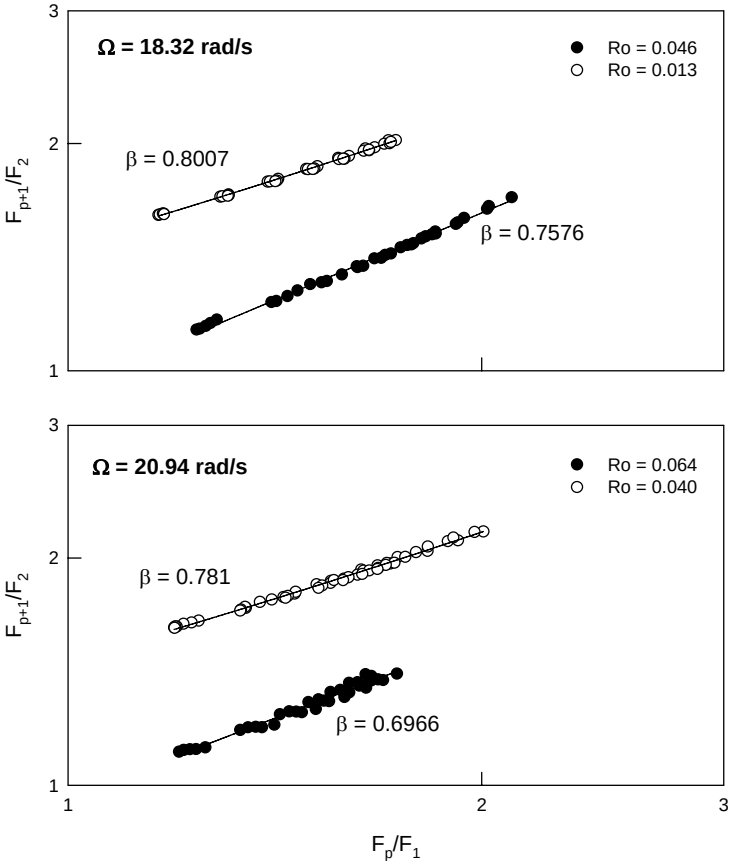

FIG. 8. β-tests for the flows in Table 1, where a straight line indicates that the data satisfy β-test.

5.2 The γ-test

The hierarchical structure model also assumes the scaling:

$$F_\infty \square S_3^\gamma(l) \tag{10}$$

where γ describes the scaling of the most intermittent structures with respect to the magnitude of more typical events (of the order of $\langle \delta u \rangle$, or $S_3^{1/3}$) [38]. When γ = 1/3, the fluctuations of all intensities are statistically alike, or the flow is globally self-

similar. When $\gamma = 0$, the magnitude of the most intermittent structures is not related to the typical fluctuation magnitude. Hence, decreasing γ indicates increasing distinction of the most intermittent structures from the background flow structures. With the assumption of Eq. (10), the scaling exponent of the velocity difference structure functions ζ_p is given as follows:

$$\zeta_p = \gamma p + C(1-\beta^p) \tag{11}$$

where $C = (1-3\gamma)/(1-\beta^3)$. Given the values of β, the validity of Eq. (10) can be tested by checking that:

$$\zeta_p - \chi(p;\beta) = \gamma[p - 3\chi(p;\beta)] \tag{12}$$

where $\chi(p;\beta) = (1-\beta^p)/(1-\beta^3)$. The plots of the γ-test are shown in Fig. 9. In the case of orbital shaker speed Ω = 18.32 rad/s, the γ value was high (γ = 0.21) at the bottom location than that at the top location (γ = 0.14) indicating that the flow was much more turbulent at the top location. At the orbital shaker speed Ω = 20.94 rad/s, the values of γ varied from 0.13 to 0.17 which indicates that intermittency was close at both the locations.

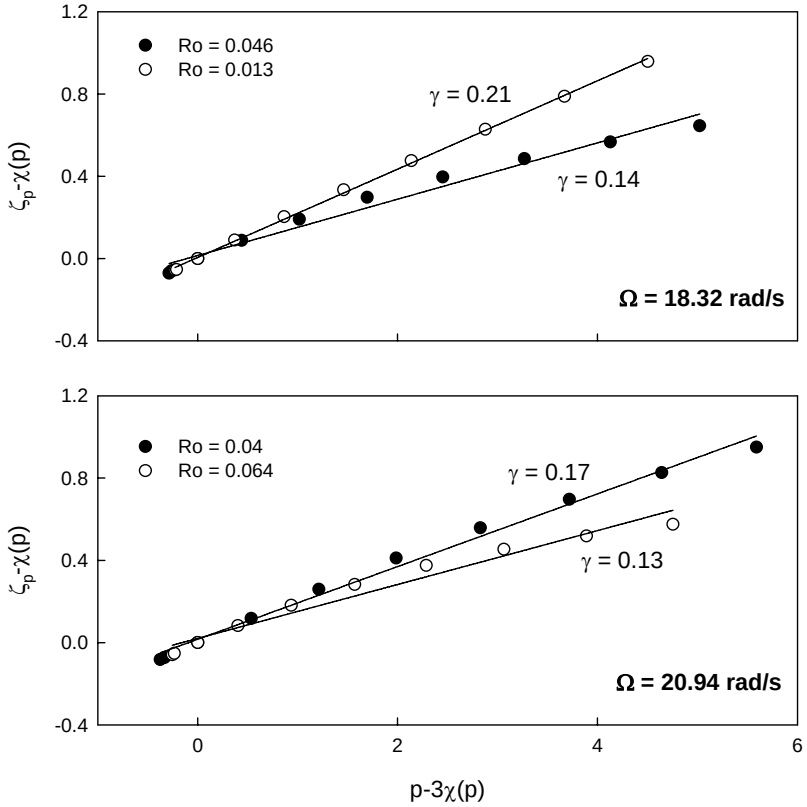

FIG. 9. γ-tests for the flows in Table 1. The straight lines are the least squares fits to the data.

6 Discussions

The statistical properties of turbulence were evaluated in eccentrically rotating Swirling flask using Hot wire Anemometer. Two orbital shaker speeds were considered and they were Ω = 18.32 and 20.94 rad/s. By examining the velocity time series, it was noticed that velocity fluctuations were dampened as one approached the bottom of the flask. This could be attributed to the larger pressure forces at the bottom of the flask. But the average velocities remained almost constant with depth. Rather these average velocities varied radially, with higher velocities away from the center. The flow looked quasi-two-dimensional at the larger scale.

When we performed the structure function analysis using Extended Self-Similarity we found that the scaling exponents ζ_p were in close accord with the prediction of the She-Leveque model except at high values of p (p >7) where the discrepancy could be attributed to less reliable statistics. Also, at Ro = 0.013 the scaling exponent curve was closer to K41 curve indicating that at low Rossby numbers the scale dependence becomes less and the flow becomes self similar. This is a characteristic of two-dimensional turbulence.

The application of the β and γ tests of the Hierarchical Structure model provided details about the structure of the flow in the SF. The value of β decreased with the increase in elevation and orbital shaker speeds, indicating highly intermittent flow at high Ω value and at Z = 3.1cm. The value of γ confirmed this observation: at high value of Ω the values of γ were smaller compared with that at low value of Ω.

All the structure function and Hierarchical Structure model analysis lead to the conclusion that the flow in the flask is 3D at the local scale while the average velocity distribution shows the flow to be quasi-two dimensional at the large scale.

Acknowledgement.
This research was supported, in part, by the U.S. Environmental Protection Agency through Contract No. PR-OH-01-00381. However, no official endorsement of the results should be implied.

References

[1] F. Anselmet, Y. Gagne, E. J. Hopfinger, and R. A. Antonia, 1984, High-order Velocity Structure Functions in Turbulent Shear Flow, J. Fluid Mech., 140 (1984), 63-89.

[2] L. C. Andrews, R. L. Phillips, B. K. Shivamoggi, J. K. Beck, and M. L. Joshi, A statistical theory for the distribution of energy dissipation in intermittent turbulence, Phys. Fluids A, 1(1989), 999-1006.

[3] A. Arneodo, C. Baudet, F. Belin, B. Castaing, B. Chabaud, R. Chavarria, S. Ciliberto, R. Camussi, F. Chilla, B. Dubrulle, Y. Gagne, B. Hebral, J. Herweijer, M. Marchand, J. Maurer, J. F. Muzy, A. Naert, A. Noullez, J. Peinke, F. Roux, P. Tabeling, W. Vand de Water, and H. Willaime, Structure Functions in Turbulence, in various flow configurations, at Reynolds number between 30 and 5000 using Extended Self-Similarity, Europhys. Lett., 34(1996), 411-416.

[4] C. N. Baroud, B. B. Plapp, H. L. Swinney, and Z. –S. She, Scaling in three-dimensional and quasi two-dimensional rotating turbulent flows, Phys. Fluids, 15(2003), 2091-2104.

[5] C. N. Baroud, B. B. Plapp, Z. –S. She, and H. L. Swinney, 2002, Anomalous Self-Similarity in a Turbulent Rapidly Rotating Fluid, Phys. Rev. Lett., 88(2002), 114501.

[6] R. Benzi, S. Ciliberto, R. Tripiccione, C. Baudet, F. Massaioli, and S. Succi, Extended Self-Similarity in Turbulent Flows, Phys. Rev. E, 48(1993), R29-R32.

[7] R. Benzi, G. Paladin, G. Parisi, and A. Vulpiani, On the multifractal nature of fully developed turbulence and chaotic systems, J. Phys., A17 (1984), 3521-3531

[8] O. N. Boratav, and R. B. Pelz, Structures and Structure Functions in the Inertial range of Turbulence, Phys. Fluids, 9(1997), 1400-1415.

[9] V. M. Canuto, and M. S. Dubovikov, Physical regimes and dimensional structure of Rotating Turbulence, Phys. Rev. Lett., 78(1997), 666.

[10] J. R. Clayton, J. R. Payne, and J. S. Farlow, Oil Spill Dispersants, Mechanical Action and Laboratory Tests, C. K. Smoley, Boca Raton, Florida, 1993.

[11] G. R. Chavarria, C. Baudet, R. Benzi, and S. Ciliberto, Hierarchy of the Velocity Structure Functions in Fully Developed Turbulence, J. Phys. II France, 5 (1995), 485-490.

[12] R. G. Dean, and R. A. Dalrymple, Water Wave Mechanics for Engineers and Scientists, Prentice-Hall, Englewood Cliffs, N. J., 1984.

[13] M. F. Fingas, Dispersants: A Review of Effectiveness Measures and Laboratory Physical Studies," Proc. Alaska RRT Dispersant Workshop, U.S. Minerals Management Service, Anchorage, Alaska, 1991.

[14] M. F. Fingas, Use of Surfactants for Environmental Applications, in Surfactants: Fundamentals and Applications to the Petroleum Industry, Laurier L. Schramm, ed., Cambridge University Press, Cambridge, UK, 461-539, 2000.

[15] H. B. Fischer, E. J. List, R. Koh, J. Imberger, and N. H. Brooks, Mixing in inland and coastal waters, Academic Press, New York, NY, 1979.

[16] U. Frisch, Turbulence: The Legacy of A. N. Kolmogorov, Cambridge University Press, Cambridge, UK, 1996.

[17] U. Frisch, and G. Parisi, Turbulence and Predictability in Geophysical Fluid Dynamics and Climate Dynamics, M. Ghil, R. Benzi, and G. Parisi, eds., North-Holland Publ. Co., 1985.

[18] A. D. Gilbert, Spiral Structures and spectra in two-dimensional turbulence, J. Fluid Mech., 193(1988), 475-497.

[19] V. J. Kaku, M. C. Boufadel, and A. D. Venosa, Evaluation of Mixing Energy in Laboratory Flasks used for Dispersant Effectiveness Testing, J. Envir. Engrg., 132(2006), 93-101.

[20] V. J. Kaku, M. C. Boufadel, A. D. Venosa, and J. Weaver, Flow Dynamics in Eccentrically Rotating Flasks used for Dispersant Effectiveness Testing, Envir. Fluid Mech., 6(2006), 385-406

[21] S. Kida, Log-stable distribution and Intermittency of Turbulence, J. Phys. Soc. Jpn., 60(1991), 5-8.

[22] A. N. Kolmogorov, The Local Structure of Turbulence in Incompressible Viscous Fluid for very large Reynolds number, Dokl. Akad. Nauk SSSR, 30(1941), 9-13.

[23] A. N. Kolmogorov, On degeneration (decay) of isotropic turbulence in an incompressible viscous liquid, Dokl. Akad. Nauk SSSR, 31(1941), 538-540.

[24] A. N. Kolmogorov, A refinement of previous hypotheses concerning the local structure of turbulence in a viscous incompressible fluid at high Reynolds number, J. Fluid Mech., 13(1962), 82-85.

[25] E. Kreyszig, Advanced Engineering Mathematics, 8th Ed., John Wiley & Sons, New York, N. Y., 1999.

[26] G. S. Lewis, and H. L. Swinney, Velocity Structure Functions, Scaling, and Transitions in high-Reynolds number Couette-Taylor flow, Phys. Rev. E, 59(1999), 5457-5467.

[27] C. Meneveau, and K. R. Sreenivasan, Simple multifractal cascade model for fully developed turbulence, Phys. Rev. Lett., 59(1987), 1424-1427.

[28] M. Nelkin, Universality and Scaling in Fully Developed Turbulence, Adv. Phys., 43(1994), 143-181.

[29] J. –F. Pinton, and R. Labbe, Correction to the Taylor hypothesis in Swirling Flows, J. Phys. II France, 4(1994), 1461-1468.

[30] Z. –S. She, and S. A. Orszag, Physical model of intermittency in turbulence: Inertial-range non-Gaussian statistics, Phys. Rev. Lett., 66(1991), 1701-1704.

[31] Z. –S. She, and E. Leveque, Universal Scaling Laws in Fully Developed Turbulence, Phys. Rev. Lett., 72(1994), 336-339.

[32] Z. –S. She, K. Ren, G. S. Lewis, and H. L. Swinney, Scalings and structures in turbulent Couette-Taylor flows, Phys. Rev. E., 64(2001), 016308.

[33] L. Smith, and F. Waleffe, Transfer of energy to two-dimensional large scales in forced, rotating three-dimensional turbulence, Phys. Fluids, 11(1999), 1608-1622.

[34] G. I. Taylor, Dispersion of soluble matter in solvent flowing slowly through a tube, Proc. Royal Soc. London, Ser. A., 219(1953), 186-203.

[35] G. I. Taylor, The dispersion of matter in turbulent flow through a pipe, Proc. Royal Soc. London, Ser. A., 223(1954), 446-468.

[36] H. Tennekes, and J. L. Lumley, A First Course in Turbulence, MIT Press, Cambridge, MA, 1972.

[37] A. Vincent, and M. Meneguzzi, The Spatial Structure and Statistical Properties of Homogeneous Turbulence, J. Fluid Mech., 225(1991), 1-25.

[38] Y. Zhou, A Phenomenological treatment of Rotating Turbulence, Phys. Fluids, 7(1995), 2092-2094.

Received: November, 2008